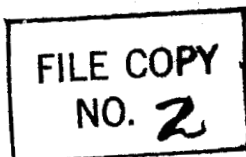


#2



N 62 57562  
**CASE FILE  
COPY**

TECHNICAL MEMORANDUMS

NATIONAL ADVISORY COMMITTEE FOR AERONAUTICS

THIS DOCUMENT ON LOAN FROM THE FILES OF

NATIONAL ADVISORY COMMITTEE FOR AERONAUTICS  
LANGLEY MEMORIAL AERONAUTICAL LABORATORY  
LANGLEY FIELD, HAMPTON, VIRGINIA

RETURN TO THE ABOVE ADDRESS.

REQUESTS FOR PUBLICATIONS SHOULD BE ADDRESSED  
AS FOLLOWS:

No. 562

NATIONAL ADVISORY COMMITTEE FOR AERONAUTICS  
1724 STREET, N.W.,  
WASHINGTON 25, D.C.

EXPERIMENTAL INVESTIGATION OF AIRCRAFT PROPELLERS

EXPOSED TO OBLIQUE AIR CURRENTS

By O. Flachsbart and G. Kröber

From Zeitschrift für Flugtechnik und Motorluftschiffahrt  
December 14, 1929

Washington  
April, 1930

NATIONAL ADVISORY COMMITTEE FOR AERONAUTICS.

---

TECHNICAL MEMORANDUM NO. 562.

---

EXPERIMENTAL INVESTIGATION OF AIRCRAFT PROPELLERS  
EXPOSED TO OBLIQUE AIR CURRENTS.\*

By O. Flachsbart and G. Kröber.

S u m m a r y

Two screw propellers, a normal airplane propeller with a pitch/diameter ratio  $H/D = 0.5$  and a helicopter propeller  $H/D = 0.2$ , were tested in the large wind tunnel of the Göttingen Aerodynamic Institute. With both propellers the angle between the propeller axis and the direction of the wind was varied from  $0$  to  $90^\circ$ . In addition to the three force and the three moment components in a wind-fast coordinate system, the corresponding components in a propeller-fast coordinate system, a total of six force and six moment components, together with the propulsive efficiency, were measured or calculated from measurements. The results are given in the form of diagrams and briefly discussed. The propeller models and method of experimentation are described and the symbols are defined.

Introduction

Under normal operating conditions any propelled craft moves so that the direction of the relative flow is exactly or very

---

\*Experimentelle Untersuchungen an schräg angeblasenen Schraubenpropellern." From Zeitschrift für Flugtechnik und Motorluftschiffahrt, December 14, 1929, pp.605-314.

nearly in the direction of the propeller axis. These conditions are the normal straightaway flight of an airplane, the vertical ascent and descent of a helicopter and the straightaway motion of a ship. Since these conditions predominate in practice, they have been made the principal objects of theoretical and experimental investigation.

All propelled craft sometimes come, however, into positions in which the direction of the relative flow deviates considerably from the direction of the propeller axis. The principal cases are:

1. Curving motion of all propelled craft. The angle between the propeller axis and the relative flow (hereinafter called the angle of flow and designated by  $\alpha$ ) is inversely proportional to the radius of the curve.

2. The horizontal flight of a helicopter, in which the horizontal motion is produced by inclining the propeller axis. On such a helicopter the propeller performs the dual function of vertical lift and horizontal propulsion. The resulting angle of flow ( $\alpha$ ) is large in comparison with case 1.

In 1914, Bramwell, Relf and Bryant, in wind-tunnel experiments with propellers exposed to oblique air currents, measured the thrust components parallel and perpendicular to the propeller axis at flow angles of  $\alpha = 0$  to  $25^\circ$  \* Similar measurements

---

\*"Experiments to Determine the Lateral Force on a Propeller in a Side Wind." British A.C.A. Reports and Memoranda No. 123, Part II.

were recently made at the Junkers factory.\* These experiments cover the angles of flow in curving motion (case 1). Of course they also cover the effect of the oblique flow in those cases in which the relative flow is generally assumed with sufficient accuracy to be axial. These cases include the straightaway flight of an airplane whose propeller axis has a direction different from the direction of flight, inverted flight, the flow relations in certain arrangements of the propeller above or below the wings and similar cases.

In order to determine the behavior of propellers under the operating conditions of case 2, Durand and Lesley investigated, in 1921, a series of propellers of different  $H/D$  ratios (0.3, 0.5, 0.7) at angles of flow of  $\alpha = 60$  to  $90^\circ$  in a wind tunnel and determined the axial thrust and the torque.\*\* Margoulis has recently investigated helicopter-propeller models in a lateral wind.\*\*\*

Since the former of the above-mentioned cases (oblique flow against airplane propellers) relates to small angles of flow and the latter (oblique flow against helicopter propellers) relates to large angles of flow and hence practically cover the range from  $\alpha = 0$  to  $90^\circ$ , and since, moreover, the quantities measured

---

\*Bock, "Ueber die Einheit von Triebwerk und Flugwerk," Year-book of the W.G.L., 1928, p.66.

\*\*Durand and Lesley, "Tests on Air Propellers in Yaw." N.A.C.A. Technical Report No. 113, 1921.

\*\*\*Margoulis, "Les hélicoptères," Paris, 1922; "Nouvelles recherches expérimentales sur les hélices d'hélicoptères," Comptes Rendus 184, 1927, p.735.

by the earlier experimenters are limited in all cases to a portion of the thrust components and moments, the authors generalized the problem according to the behavior of a propeller in a side wind and undertook the task of investigating screw propellers of different pitch in the wind tunnel at angles of flow of 0 to  $90^\circ$ . In addition to the propulsive efficiency, all forces and moments in a wind-fast system and in a propeller-fast system of coordinates were to be investigated.

### The Propellers Tested

Two propeller models of the same diameter  $D$ , but of different pitch  $H$ , were tested.

1. An airplane propeller model of uniform pitch  $H = 0.5 D$  throughout the whole radius (Fig. 1). The propeller was of the type  $S_1 F_2 A_1 P_1$  of the N.A.C.A. reports.\*

2. A helicopter propeller with a uniform pitch of  $H = 0.2 D$  over the greater (outer) part of the radius (Fig. 2).

The diameter of both propellers was  $D = 0.32$  m (12.6 in.). They were made from a block of glued strips of wood, like full-size propellers. In reporting the results, the propellers are simply designated as I and II.

---

\*Durand and Lesley, "Experimental Research on Air Propellers-V." N.A.C.A. Technical Report No. 141, 1925.

## Suspension of Model

Both propeller models were tested in the large wind tunnel of the Göttingen Aerodynamic Institute. A small high-speed Göttingen electric motor of the type C was used to drive them.\* The suspension in the wind tunnel is shown in Figures 3 and 4. The plane, in which the propeller axis can be adjusted, is the vertical plane of symmetry of the air stream. In only one case, in measuring the vertical moment, was it necessary, for technical reasons, to mount the propeller so it could be tilted in the middle horizontal plane of the air stream (Fig. 5). Before considering the experiments we must define the forces and moments.

## Definitions and Notation

We will first express all the forces and moments as nondimensional and will use the following formulas.

Force or thrust coefficient

$$k_s = 100 \frac{\text{force}}{\frac{\rho}{2} \left(\frac{D}{2} \omega\right)^2 \frac{D^2 \pi}{4}}$$

Moment coefficient\*

$$k = 100 \frac{\text{moment}}{\frac{\rho}{2} \left(\frac{D}{2} \omega\right)^2 \frac{D^2 \pi}{4} \frac{D}{2}}$$

---

\*"Ergebnisse der Aerodynamischen Versuchsanstalt zu Göttingen," Report III, 1927.

\*\*These coefficients are 100 times those ordinarily used in propeller aerodynamics. It is customary to employ the propeller coefficients, like the wing coefficients, as 100 times the ordinary coefficients, on account of the smallness of the latter (e.g., 100  $c_a$  and 100  $k_d$ ). In order not to be obliged to use this numerical factor 100 in the numerous diagrams in which the test re- (For remainder of footnote, see bottom of page 6.)

- $\rho$ , density of surrounding medium ( $\text{kg s}^2 \text{m}^{-4}$ );
- $D$ , propeller diameter (m);
- $\omega$ , angular velocity of propeller  $\pi n/30$ , when  
     $n = \text{its r.p.m. (s}^{-1}\text{)}$ .

In order to save trouble, it is allowable, instead of speaking of the force and moment coefficients  $k_s$  and  $k$ , simply to say the force (or thrust)  $k_s$  and the moment  $k$ .

All components are designated by a subindex. Since the thrust symbol already has the subindex  $s$ , we can easily distinguish the thrust forces and moments by using two subindices (e.g.,  $k_{s_n}$  for the thrusts and only one for the moments (e.g.,  $k_d$ ).

Let us now imagine (Figs. 6-7) a wind-fast right-hand orthogonal system of axes  $XYZ$  so oriented that the  $X$  axis is in the direction of flow and the  $XZ$  plane is the vertical plane of symmetry in the air stream. With this system of axes we combine the propeller-fast system of axes  $X'Y'Z'$  in such manner that the axis around which the propeller swings (the  $Y'$  axis) coincides with the  $Y$  axis. The adjustment plane of the propeller (the  $X'Z'$  plane) then lies in the  $XZ$  plane. Hence we can convert the wind-fast system of axes  $XYZ$  into the propeller-fast system of axes  $X'Y'Z'$  by rotation about the  $Y$  axis by the angle of flow  $\alpha$ .

According to this definition of the system of axes, the forces and moments, exerted on the propeller by the air, are as

---

(Continued from page 5)  
sults are shown, the authors decided to use the above modified formula.

follows.

Wind-fast system of coordinates XYZ.

Forces:

$k_{sh}$ , horizontal thrust (thrust component in X direction);  
 $k_{sv}$ , vertical " ( " " " Z " );  
 $k_{ss}$ , lateral " ( " " " Y " ).

Moments (with reference to the axis point of the forward tangential plane of the propellers - Figures 1-2):

$k_q$ , lateral moment (moment about an axis in the direction of flow = moment about the X axis);  
 $k_k$ , moment of yaw (moment about vertical axis = moment about Z axis);  
 $k_h$ , vertical moment (moment about swing axis = moment about Y axis).

Propeller-fast System of Coordinates X'Y'Z'

Forces:

$k_{sa}$ , axial thrust (thrust in the direction of the propeller axis = thrust in X' direction);  
 $k_{sn}$ , normal thrust (thrust in Z' direction);  
 $k_{ss}$ , lateral " ( " " Y' " ).



Moments (with reference to the axis point of the forward tangential plane of the propellers, Figs. 1-2):

$k_r$ , moment of roll (moment about the propeller axis = moment about  $X'$  axis);

$k_g$ , moment of yaw (moment about  $Z'$  axis);

$k_h$ , vertical moment (moment about  $Y'$  axis).

The fact that the lateral thrust  $k_{s_g}$  and the vertical moment  $k_h$  coincide in both coordinate systems, is due to the identity of the  $Y$  and  $Y'$  axis.

The rolling moment  $k_r$  exerted on the propeller by the air forces, is obviously equal and opposite to the turning moment transmitted from the motor to the propeller. This turning moment is expressed by  $k_d$  in the usual manner. Therefore, if we define the positive  $k_d$  direction in opposition to the positive  $k_r$  direction,  $k_r = k_d$  in every direction.

Moreover, if we define the efficiency of propulsion

$$\eta = \frac{k_{s_h}}{k_d} \lambda,$$

in which  $\lambda$  = velocity of flow  $v$ /peripheral velocity of blade points  $u$  = pitch angle of propeller.

#### Experimental Method

The measured forces and moments are compared in the following survey. The accompanying numbers refer to the wires leading

from the model to the balances in Figure 3. They show how the quantities in question are measured.

Measured thrust components:

$k_{sv}$ , vertical thrust . . . . .	(3 + 4) + 5
$k_{sh}$ , horizontal " . . . . .	1 + 2
$k_{ss}$ , lateral " . . . . .	6

Measured moments:

$k_d (= k_r)$ , turning moment (= rolling moment) . . .	7
$k_q$ , lateral moment . . . . .	3 - 4
$k_h$ , vertical moment, measured with special suspension.	

As shown in Figure 5, the plane of adjustment in the horizontal plane of the wind tunnel was such that the vertical moment could be measured by 1 - 2.

The propeller speed, which averaged about 6500 r.p.m., was determined by the observation of a rotating mark actuated by the motor with a reduction of 1 : 400 and designated by 8 in Figure 3.

In order to be able to eliminate the effect of the motor and of the suspension in the evaluation of the measurements, a comparative test had to be made without the propeller for all quantities excepting the turning moment and r.p.m. The desired quantity is then found from the difference between the main measurement (with propeller) and the comparative measurement (without propeller). This difference, which is unavoidable in

all force measurements in wind tunnels when the action of the air forces on only a portion of the whole installation (on the model alone) is to be studied, can, with the means now at our disposal, be determined with satisfactory accuracy for models at rest. There are unavoidable errors in the investigation of independently running propellers, as always in the investigation of moving models, since parts of the installation, whose resistance is supposed to be eliminated by the comparative measurement, lie in the accelerated slipstream of the propeller, while exposed to a flow of less velocity in the comparative test. The result is a greater or smaller deviation of the measured quantities from the actual data of the isolated propeller. Recent propeller-model testing stands render it possible to keep this deviation very small in testing propellers exposed to axial currents. Since, in our investigations with a lateral wind, the installations were necessarily more bulky, it was to be expected that the deviations would increase. A control test for  $\alpha = 0^\circ$  on the propeller-testing stand showed, however, that they are generally small (Fig. 8). These deviations are negligible in the comparison of the propeller curves obtained at different angles of flow.

During the first tests it was found necessary to measure the three quantities separately:

1. The lateral thrust  $k_{ss}$ , since the torque wire 7 in Figure 3 disturbed the measurement. (It was removed for the

measurement of  $k_{s_s}$ );

2. The lateral moment  $k_q$ , since the arrangement of the balances prevented the simultaneous measurement of  $k_q$  and  $k_{s_v}$ ;

3. The vertical moment  $k_h$ , which can be computed from  $k_{s_v}$  and  $k_{s_h}$ , but only inaccurately, since small discrepancies necessarily occur in measuring large quantities and the results are therefore considerably scattered. It was therefore preferred to determine  $k_h$  with the aid of a special experimental suspension (For this purpose the adjustment plane of the propeller axis had to be located in the middle horizontal plane of the wind tunnel).

The whole series of experiments was therefore divided as follows:

Simultaneous measurements of vertical thrust  $k_{s_v}$ , horizontal thrust  $k_{s_h}$ , and turning moment (torque)  $k_d$ ;

Separate measurements of lateral thrust  $k_{s_s}$ , lateral moment  $k_q$  and vertical moment  $k_h$ .

In measuring the lateral thrust, there were strong disturbances of the flow about the motor and consequent strong lateral oscillations of the motor-propeller assembly. These ceased, however, when two vertical guide surfaces were installed on the upper side of the motor.

It was the intention of the authors to measure many components directly and to calculate only those ( $k_{s_a}$ ,  $k_{s_n}$ ,  $k_g$ )

which could not be measured due to the arrangement of the balances.

In general, the measurements proved feasible as planned, although there were technical difficulties in individual cases due to the smallness of the forces. All the vectors from the  $X$  and  $X'$  directions disappear (on account of the symmetry) at  $\alpha = 0^\circ$ . Hence they are very small at small angles of flow. Only the measurement of the moment of yaw  $k_k$  failed on account of these difficulties. This was determined graphically from  $k_r$  and  $k_q$ . Figure 7 shows the vectorial relations of the three quantities.

#### Evaluation of the Measurements and Representation of the Results

In the evaluation of the test results it was found that the measurements for small forces varied considerably. Most of the the measured curves were therefore determined twice in the following manner:

1. The balance readings were made nondimensional without regard to the comparative test, with  $\alpha$  plotted as parameter against  $\lambda$  and the scatterings averaged by eye.
2. From these curves the corrected test values were taken for a given value of  $\lambda$  and plotted against  $\alpha$ . After another averaging of the now much smaller variations, the test values were again plotted backward against  $\lambda$ .

With these mean values, further calculations were made, the comparative measurements and calibration were introduced, etc. This double plotting was found necessary for  $k_{sh}$ ,  $k_{sv}$ ,  $k_d$ , and  $k_q$ , while  $k_{sa}$  and  $k_h$  could be measured directly.

Altogether there were measured:

Forces:  $k_{sh}$ ,  $k_{sv}$ , and  $k_{sa}$ ;

Moments:  $k_q$ ,  $k_h$ , and  $k_d = k_r$ .

The thrust forces  $k_{sa}$  and  $k_{sh}$  were graphically determined from the measured forces  $k_{sv}$  and  $k_{sh}$ . The geometrical relation of the vectors is shown by Figure 6. Moreover, the moments  $k_k$  and  $k_g$  (Fig. 7) were obtained from the graphic combination of the measured moments  $k_r$  and  $k_q$ . Lastly, the efficiency

$$\eta = \frac{k_{sh}}{k_d} \lambda,$$

was calculated, so that altogether the following quantities were determined mathematically:

Forces:  $k_{sa}$  and  $k_{sh}$ ;

Moments:  $k_k$  and  $k_g$ ;

Efficiency:  $\eta$  :

Figures 9-30 represent all the force and moment components and the efficiency for propellers I and II, both as plotted against the pitch angle  $\lambda$  with the flow angle  $\alpha$  as parameter and against  $\alpha$  with  $\lambda$  as parameter. On account of the equality  $k_d = k_r$ , the latter was not plotted, but only the torque  $k_d$ .

exception of Figure 8, the introduction of the measuring points was omitted for the sake of clearness.

In the somewhat arbitrary elimination of the scattering by the above-described double averaging, controls were desired for the individual components. Hence the following connections derived from the geometric relations (Figs. 6-7) were investigated and confirmed.\*

For the forces:

For  $\lambda = 0$ ,  $k_{s_n}$  must disappear at all oblique angles of flow and  $k_{s_a}$  assume the value

$$k_{s_a} = \sqrt{k_{s_v}^2 + k_{s_h}^2} = \text{constant}$$

For  $\alpha = 0^\circ$ ,  $k_{s_v} = 0$ ,  $k_{s_n} = 0$ , and  $k_{s_s} = 0$  at all pitch angles;

For  $\alpha = 90^\circ$ ,  $k_{s_n} = -k_{s_h}$  and  $k_{s_a} = k_{s_v}$  at all pitch angles.

For the moments:

For  $\lambda = 0$ ,  $k_g$  and  $k_h$  must disappear for all angles of flow and  $k_r (= k_d)$  must assume the value

$$k_r = \sqrt{k_k^2 + k_q^2} = \text{constant}$$

For  $\alpha = 0^\circ$ ,  $k_h$  and  $k_g$  become zero at all pitch angles;

For  $\alpha = 90^\circ$ ,  $k_k = k_r (= k_d)$  and  $k_g = -k_q$  at all pitch angles.

---

\*Moreover, we have compared our results, so far as possible, with the results of previous experimenters and found the agreement good. Perhaps there will be opportunity to compare our experimental results with the theoretical results of Pistolesi and Misztal.

## Remarks on the Results

The most important points concerning the relations of the individual components were mentioned in the preceding section. It only remains to consider the results (Figs. 9-30). It must be assumed in advance that the effect of the obliqueness of the flow on the behavior of the propeller, in the region of  $0^\circ < \alpha < \text{about } 15^\circ$ , is negligible both for airplane propellers and for helicopter propellers. A comparison of the corresponding curves for airplane and helicopter propellers show an extensive agreement in their character. The diagrams must be examined for details. Attention is called to the following points.

Thrusts  $k_{s_a}$ ,  $k_{s_v}$ ,  $k_{s_h}$ ,  $k_{s_n}$ ,  $k_{s_s}$

$k_{s_a}$  - The constant axial thrust at  $\lambda = 0$  decreases with the pitch angle at small angles of flow  $\alpha$  and increases at larger angles  $\alpha$  with the pitch angle. There is an intermediate region, at  $\alpha = \text{about } 70 \text{ to } 80^\circ$ , in which  $k_{s_a}$  (as also  $k_{s_s}$ ) is almost independent of the pitch angle (Figs. 9-10).

$k_{s_v}$  - Since the axial thrust  $k_{s_a}$  is negative at large  $\lambda$ , the vertical thrust  $k_{s_v}$  is also negative at small angles of flow  $\alpha$ . The vertical thrust  $k_{s_v}$  becomes positive again at large angles of flow, since the axial velocity is smaller, and the axial thrust consequently becomes positive again (Figs. 11-12).



$k_{sh}$  - For similar reasons it follows, in agreement with the test results, that in the region of large  $\lambda$ , the horizontal thrust at small angles of flow is negative, while it is positive at large angles of flow. At  $\alpha = 90^\circ$ , there is only resistance (Figs. 13-14).

$k_{sn}$  - The normal thrust increases both with the pitch angle and with the angle of flow. Only at small  $\lambda$  the initial increase at large angles ( $\alpha > 45^\circ$ ) recedes. The forces are much smaller than those previously mentioned, the maximum value being only  $k_{sn} = 0.8$ . For the sake of clearness the curves were plotted so that the scale is five times as great as for  $k_{sa}$ ,  $k_{sv}$ , and  $k_{sh}$  (Figs. 15-16).

$k_{ss}$  - The lateral thrust is still smaller, its maximum value for the airplane propeller being only  $k_{ss} = 0.5$ ; and for the helicopter propeller only  $k_{ss} = 0.4$ . There is a strong increase with the pitch angle, increasing at first with the angle  $\alpha$ , then dropping to zero at about  $\alpha = 85^\circ$  and then becoming negative. The scale of the diagram is likewise enlarged fivefold (Figs. 17-18).

Moments  $k_d$ ,  $k_h$ ,  $k_k$ ,  $k_q$ ,  $k_g$

$k_d$  - While for  $\lambda = 0$  there is naturally no dependence of the rolling moment on the angle of flow, at large pitch angles the moment increases rapidly with increasing angle of flow, and

at  $\alpha > 50^\circ$  the moment measured in the stand test does not recede again (Figs. 19-20).

$k_h$  - The vertical moment shows a surprisingly uniform increase both with the angle of flow and with the pitch angle (Figs. 21-22).

$k_k$  - The dependence of the moment of yaw on the pitch angle is only slight. More pronounced is the increase with the angle of attack (approximately as the sine) (Figs. 23-24).

$k_q$  - The lateral moment at  $\alpha = 0^\circ$  follows the course of the rolling moment. At  $\alpha = 90^\circ$  it is identical with the negative moment of yaw, the transition being gradual (Figs. 25-26).

$k_g$  - The moment of yaw shows quite a uniform dependence on the angle of pitch. With increasing angle of attack it becomes negative after an initial increase (Figs. 27-28).

#### E f f i c i e n c y

$\eta$  - For an airplane propeller the efficiency of propulsion attains a maximum of almost 75%. Since, as referred to like ordinates of the  $k_{sh}$  and  $k_d$  curves, smaller pitch angles of helicopter propellers correspond to larger ones of airplane propellers, the propulsive efficiency, which is a function of the pitch angle, is smaller for the helicopter propeller, the maximum value of  $\eta$  being about 0.48 for the latter. For simple hel-

icopter propellers  $-\alpha = 0^\circ$  and  $\lambda = 0$  -, from which no work of transportation is required, the propulsive efficiency = 0 according to our definition (Figs. 29-30).

For estimations it is of advantage to know that, in plotting against  $\lambda$  in an angular range of  $0^\circ < \alpha < \text{about } 45^\circ$ ,\* the  $k_{s_a}$  curves have approximately equal ordinates for equal values  $\lambda \cos \alpha$ . The same statement holds true for  $k_d$ . In the above-mentioned angular range, we can therefore convert the  $k_{s_a}$  and  $k_d$  curves measured for  $\alpha = 0^\circ$  into the corresponding curves for any angle of flow  $\alpha_1$ , by multiplying their abscissas by  $\frac{1}{\cos \alpha_1}$ .\*\* Since the normal and lateral components of the propeller thrust can be disregarded in the first approximation and it may therefore be assumed that the resulting propeller thrust is in the propeller axis even at  $\alpha \neq 0^\circ$  and is therefore identical with  $k_{s_a}$ , this method of calculation enables the determination of the quantities  $k_{s_a}$ ,  $k_{s_v}$ ,  $k_{s_h}$ ,  $k_d$  and  $\eta$ , for any values of  $\alpha$  within the limits  $0^\circ < \alpha < \text{about } 45^\circ$ , from the measured axial thrust and torque for  $\alpha = 0$ , for propellers of not too great pitch.

---

\*The upper limit falls with increasing pitch of the propeller. For the helicopter propeller II,  $60^\circ$  might be allowed for the upper limit, but  $45^\circ$  is fully high enough for the airplane propeller I.

\*\*Or, which amounts to the same thing, the  $k_{s_h}$  curve, since  $k_{s_a}$  and  $k_{s_h}$  are identical at  $\alpha = 0$ .

Translation by Dwight M. Miner,  
National Advisory Committee  
for Aeronautics.

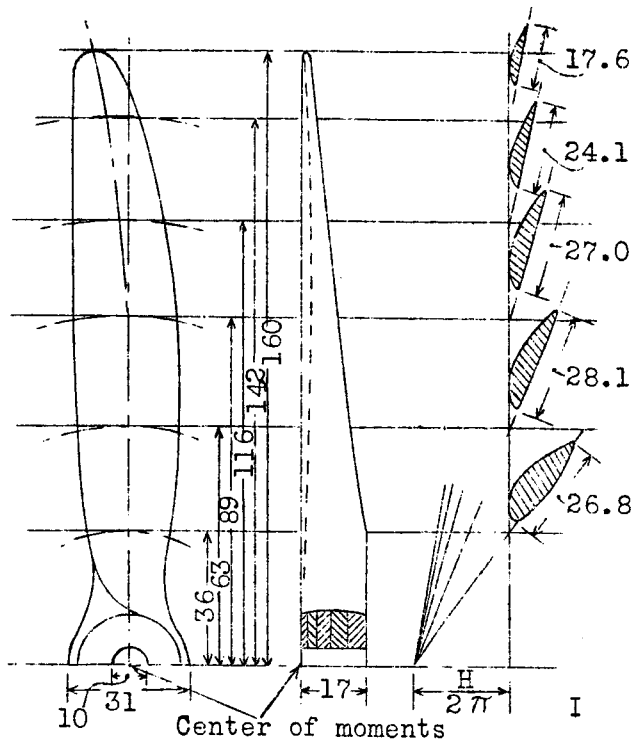


Fig.1 Airplane propeller  
(All measurements  
in mm).

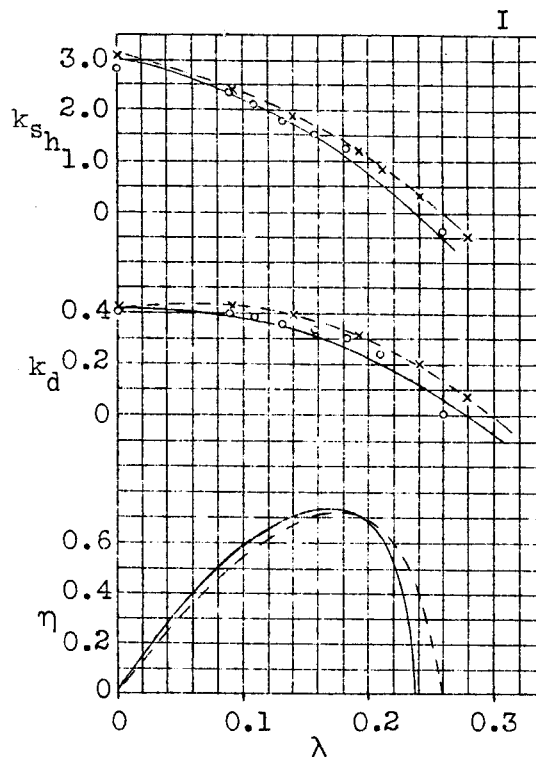
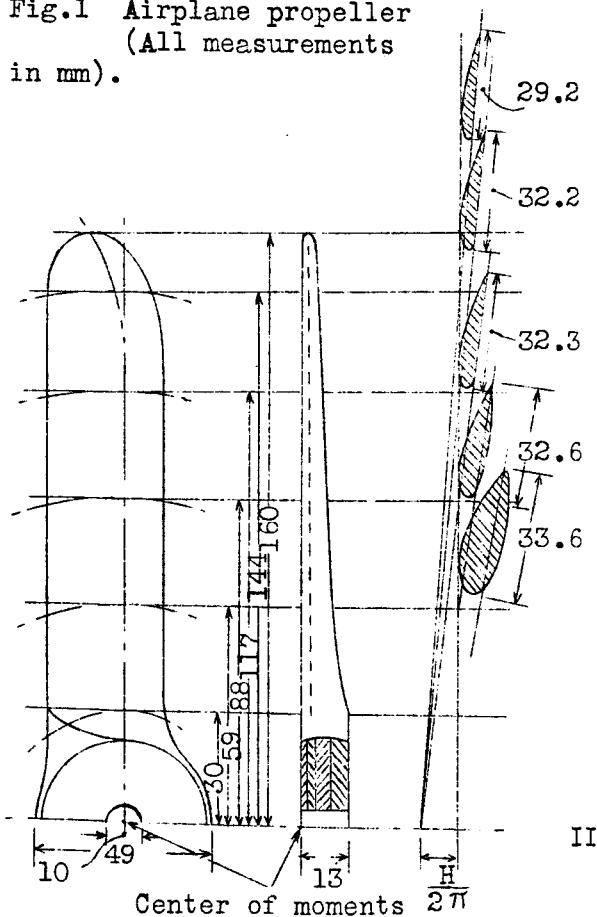


Fig.8 Effect of support on test  
results. (Airplane prop. I  
at  $\alpha=0^\circ$ )

Fig.2 Helicopter propeller.  
(All measurements  
in mm).

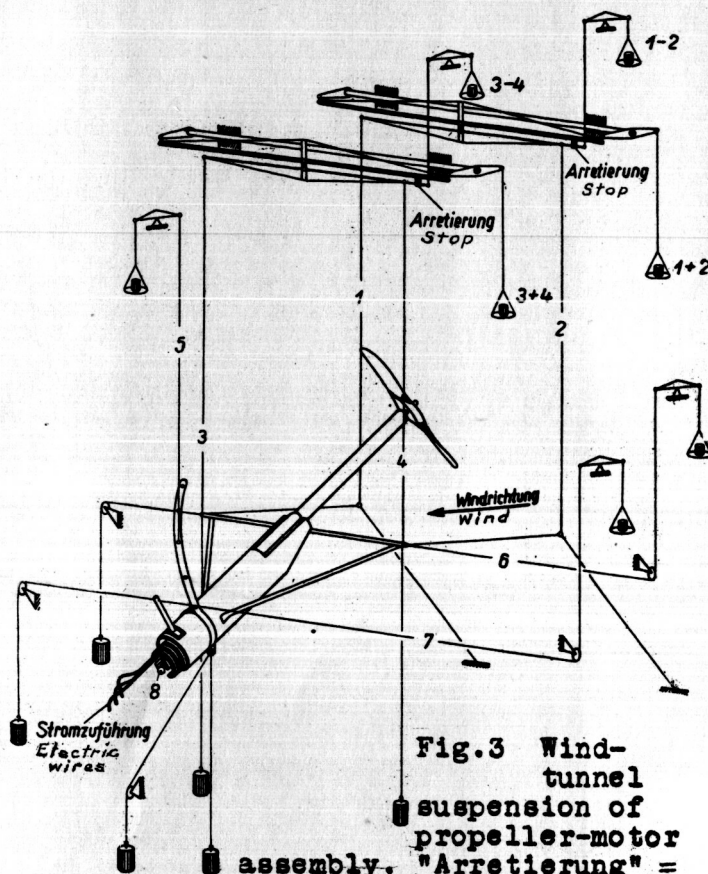


Fig.3 Wind-tunnel suspension of propeller-motor assembly. "Arretierung" =

stop. "Windrichtung" = direction of wind. "Stromzuführung" = electric wires.

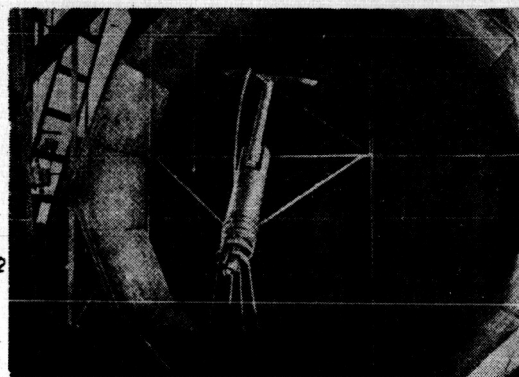


Fig.4 Wind-tunnel suspension of propeller-motor assembly.

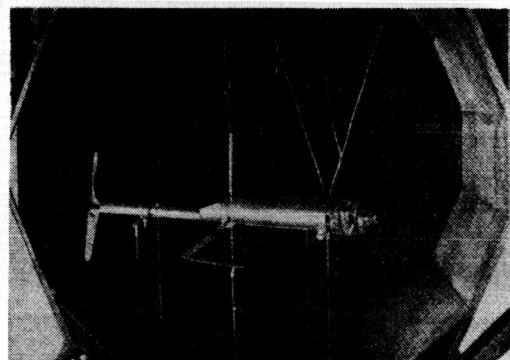


Fig.5 Special suspension for measuring vertical moment  $k_h$ .

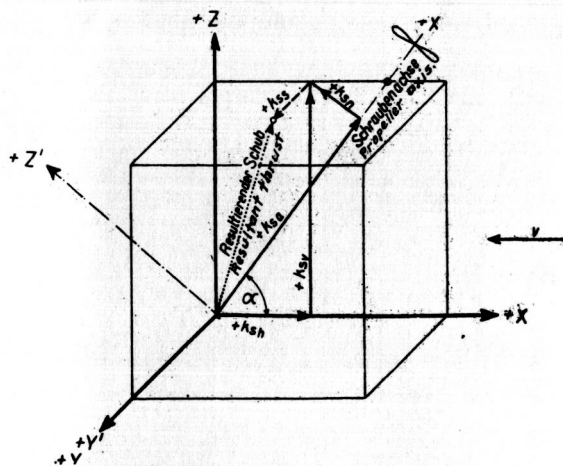


Fig.6 Thrust force.

The propeller axis lies in the XZ plane. The force vectors lie in the same plane. The dot and the dash vector fall out of the XZ plane. The cube is drawn in order to facilitate the spatial representation. Its edges were arbitrarily given a value of  $k_{sv}$ .

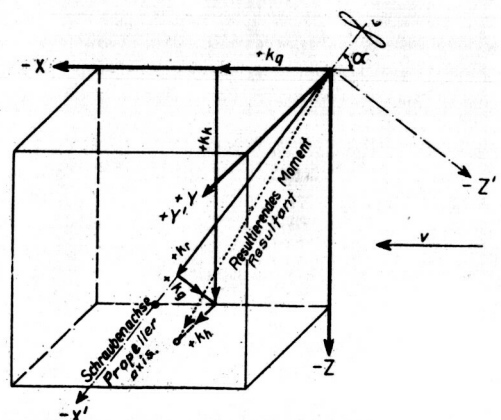


Fig.7 Moments.

The moment vectors are drawn in the usual way, so that the direction of motion indicated by the arrow, combined with the direction of rotation of the moment, produces a rotation to the right. The propeller axis lies in the XZ plane, as also the extended moment vectors. The dot and the dash vectors fall out of the XZ plane. The length of an edge of the cube is  $k_k$ .

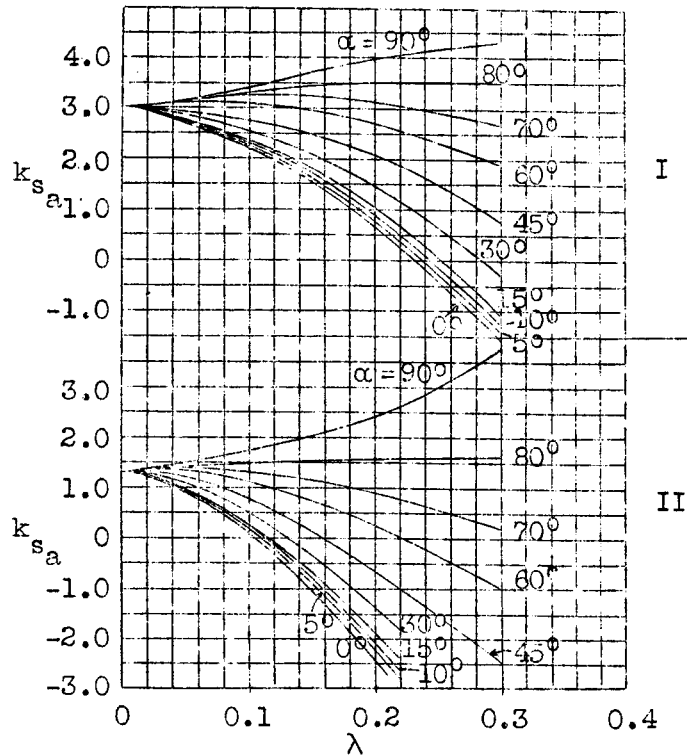


Fig.9  
Axial thrust  
plotted  
against  $\lambda$

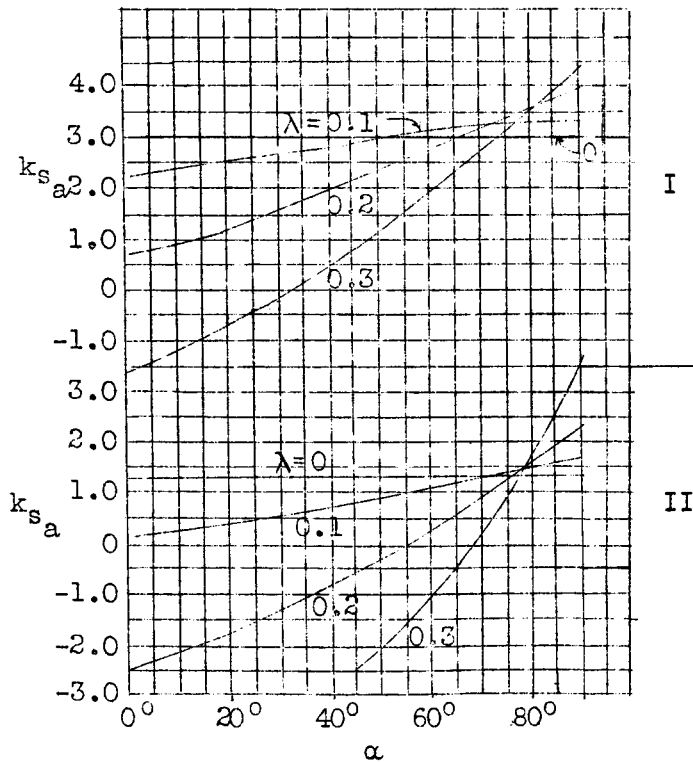


Fig.10  
Axial thrust  
plotted  
against  $\alpha$

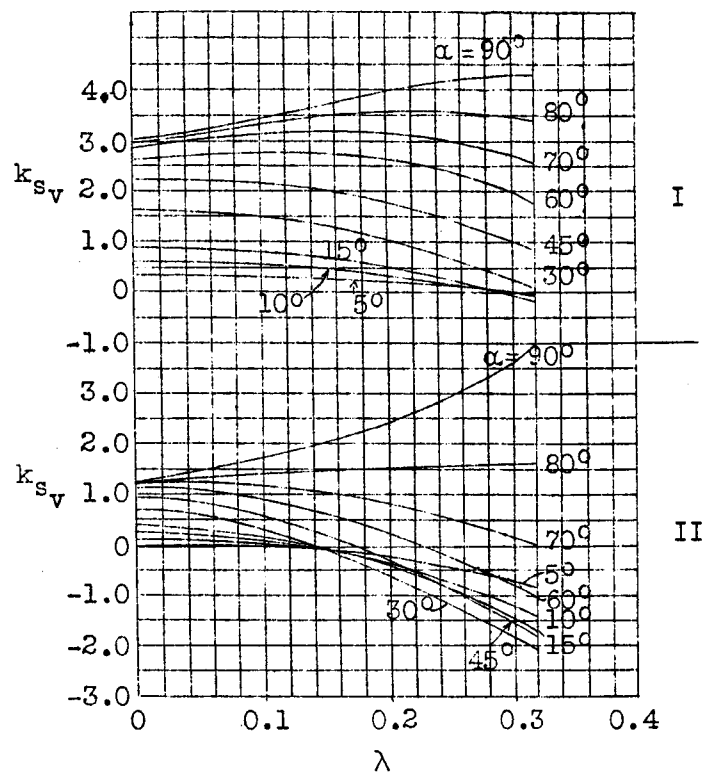


Fig.11  
Vertical thrust  
plotted against  
 $\lambda$

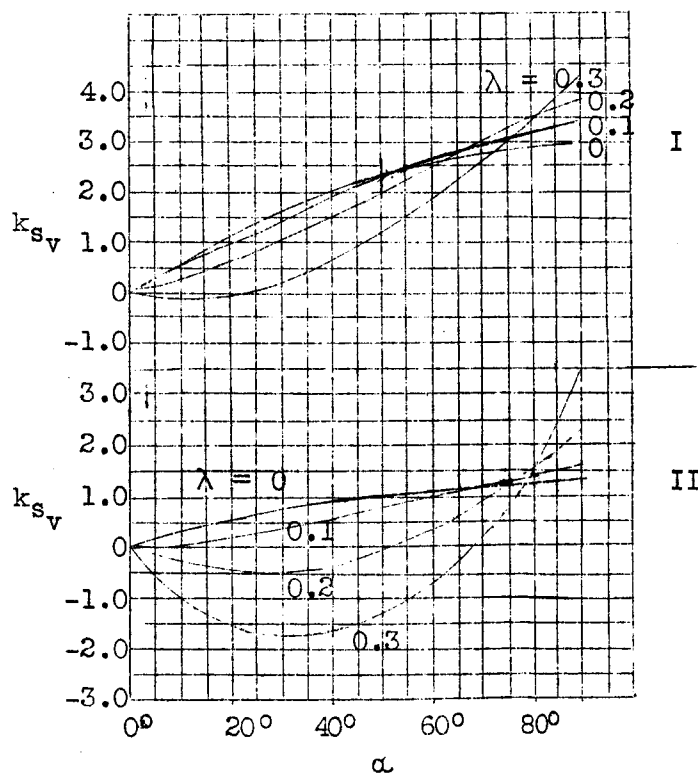


Fig.12  
Vertical thrust  
plotted against  
 $\alpha$

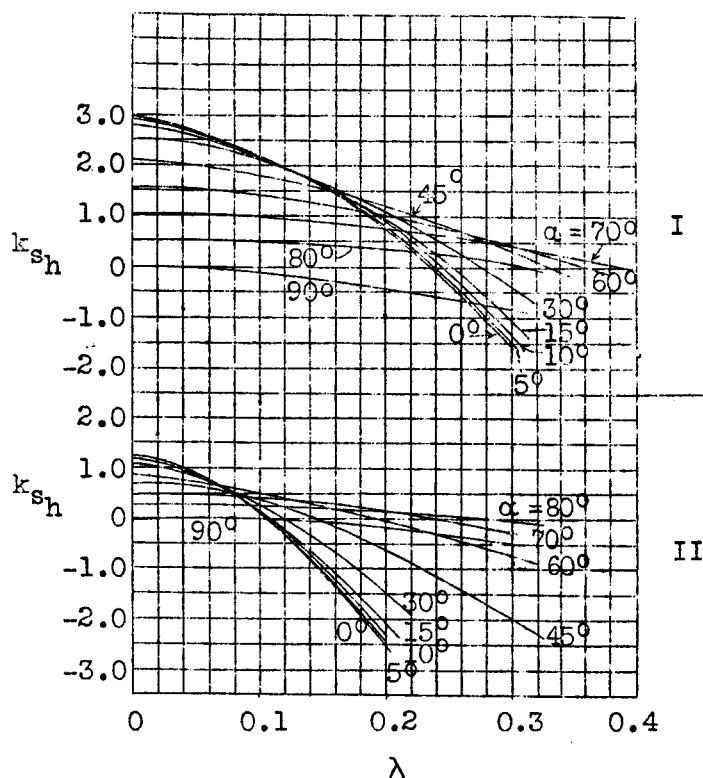


Fig.13  
Horizontal thrust  
plotted against  
 $\lambda$

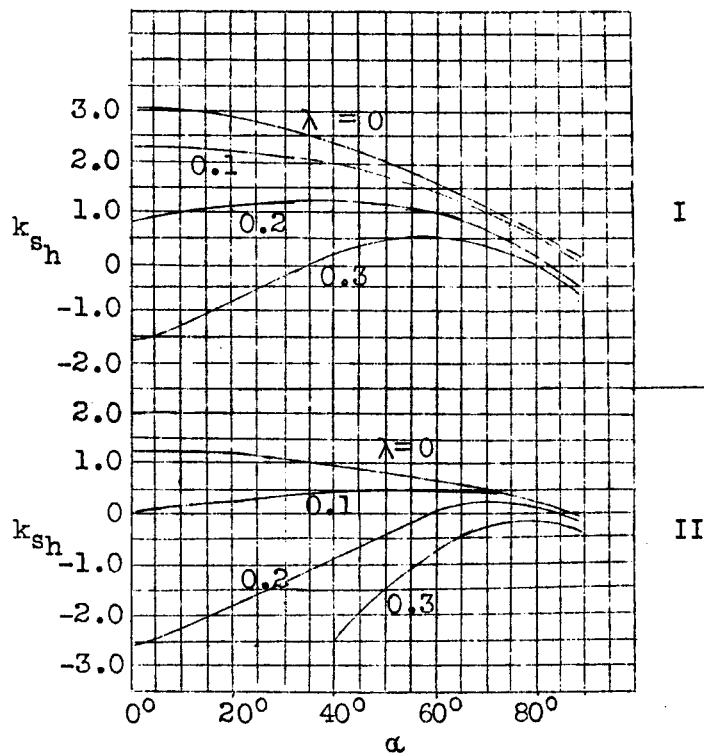


Fig.14  
Horizontal thrust  
plotted against  
 $\alpha$



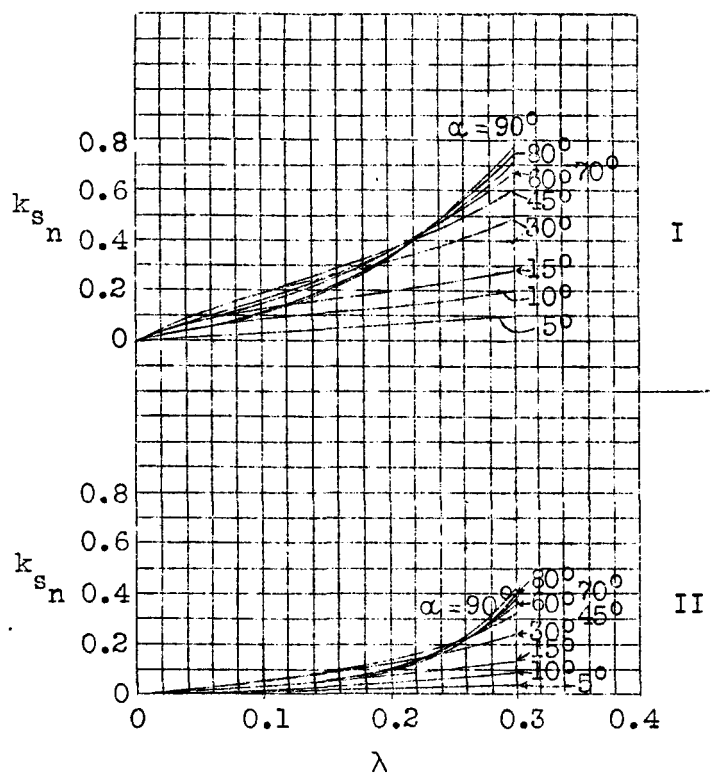


Fig.15  
Normal thrust  
plotted against  
 $\lambda$

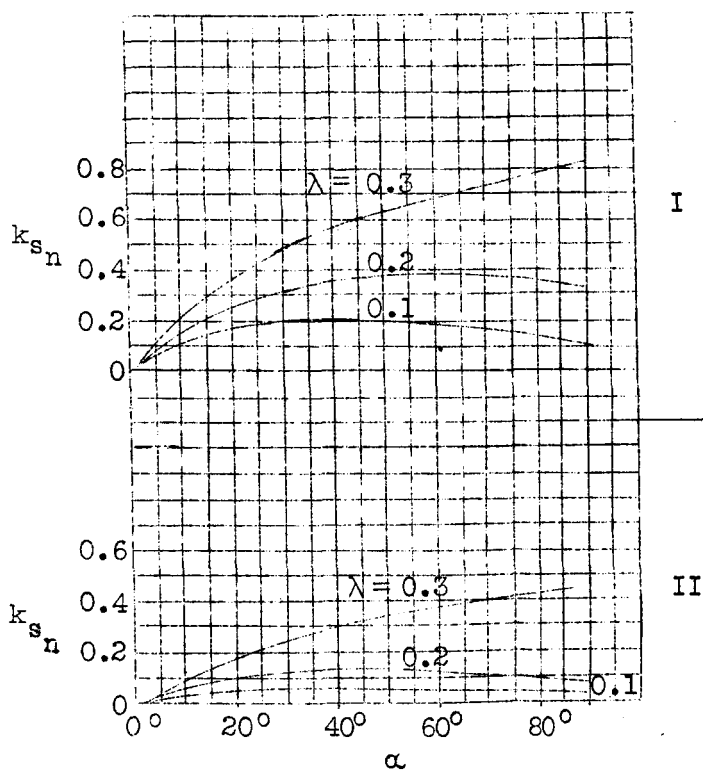


Fig.16  
Normal thrust  
plotted against  
 $\alpha$

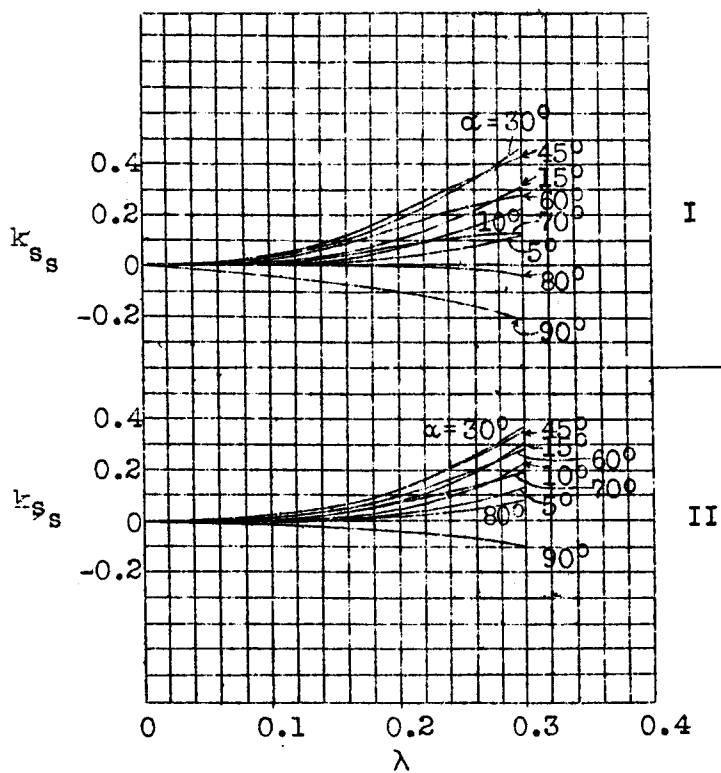


Fig.17  
Lateral thrust  
plotted against  
 $\lambda$

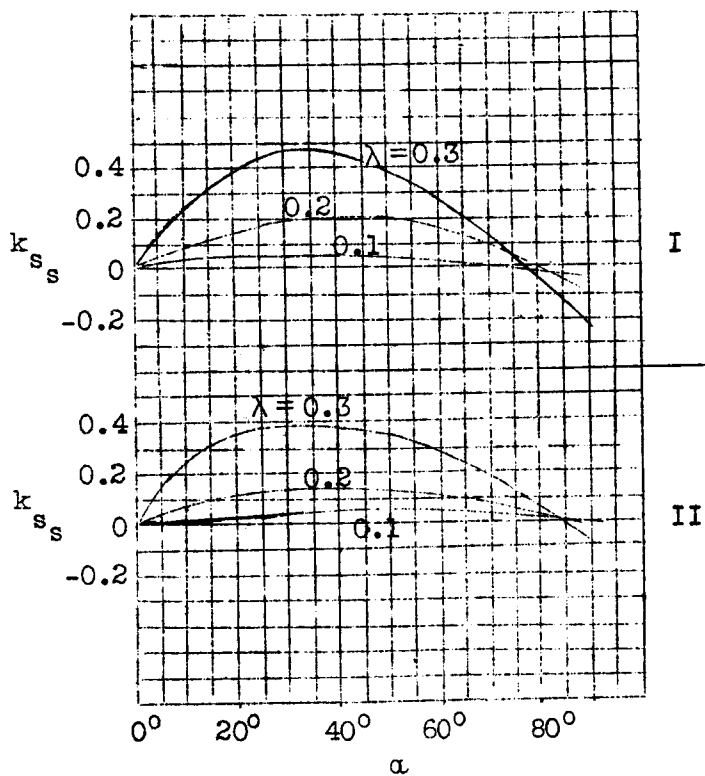


Fig.18  
Lateral thrust  
plotted against  
 $\alpha$

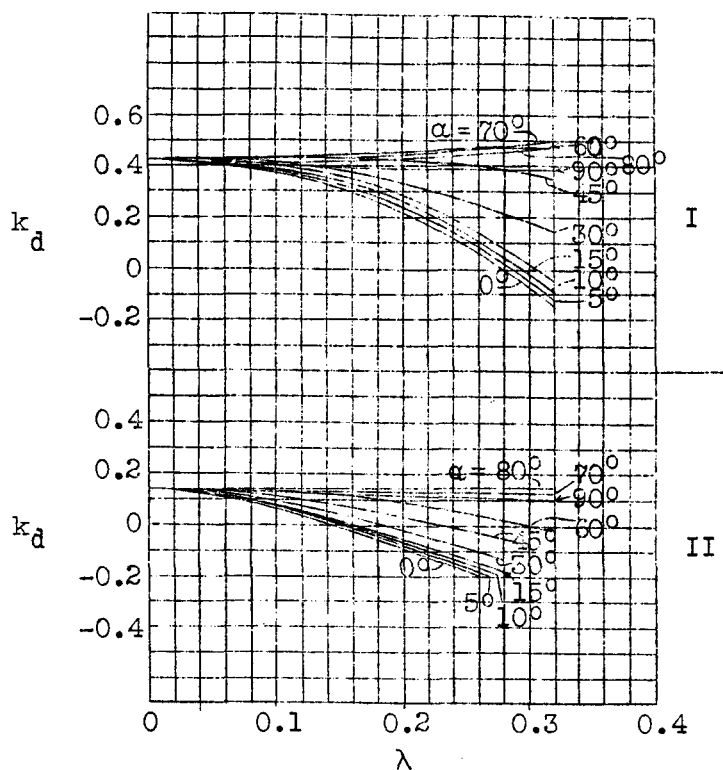


Fig.19  
Torque moment  
plotted against  
 $\lambda$

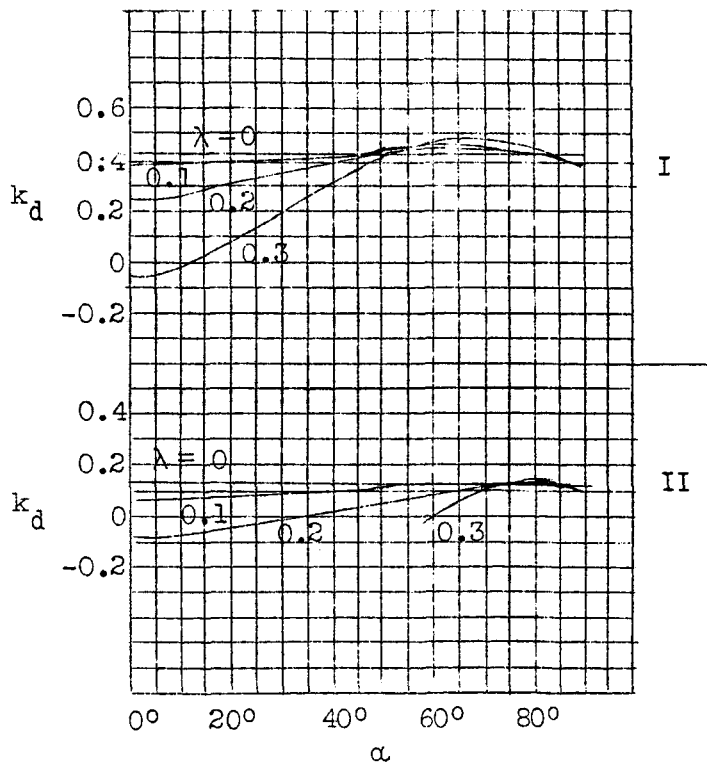


Fig.20  
Torque moment  
plotted against  
 $\alpha$

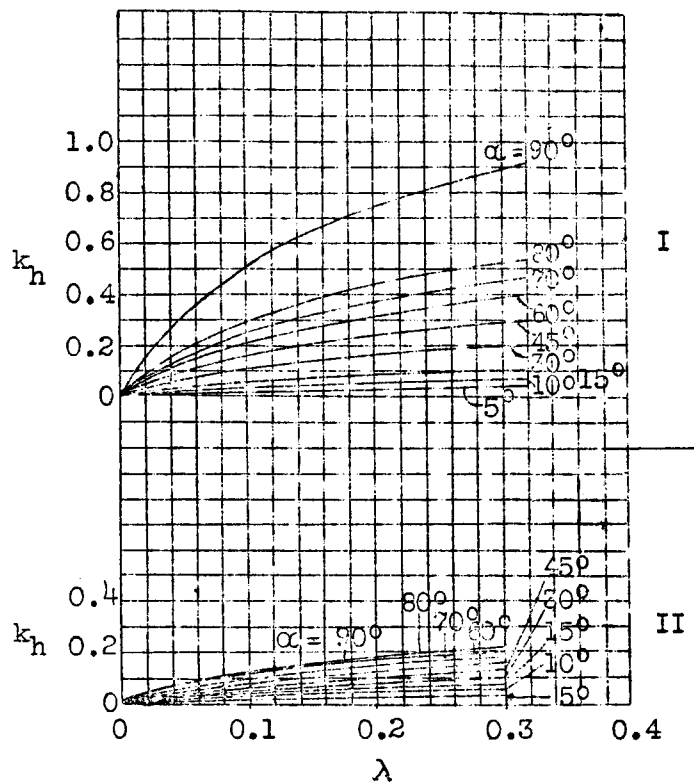


Fig.21  
Vertical moment  
plotted against  
 $\lambda$

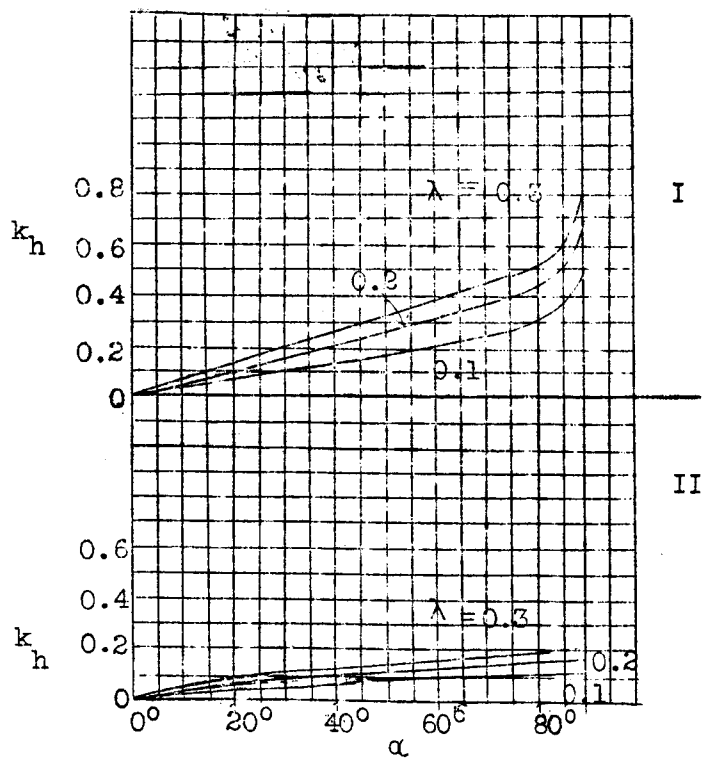


Fig.22  
Vertical moment  
plotted against  
 $\alpha$

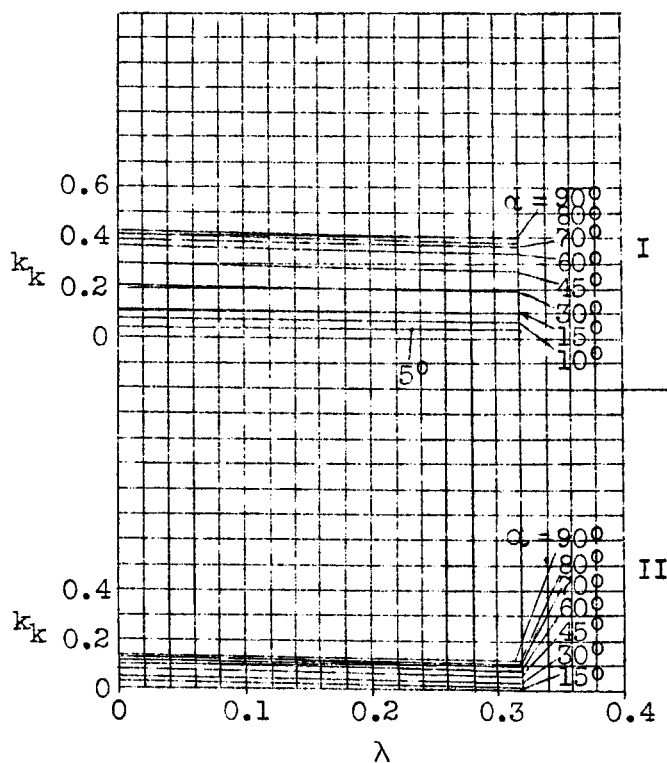


Fig.23  
Moment of yaw  
plotted against  
 $\lambda$

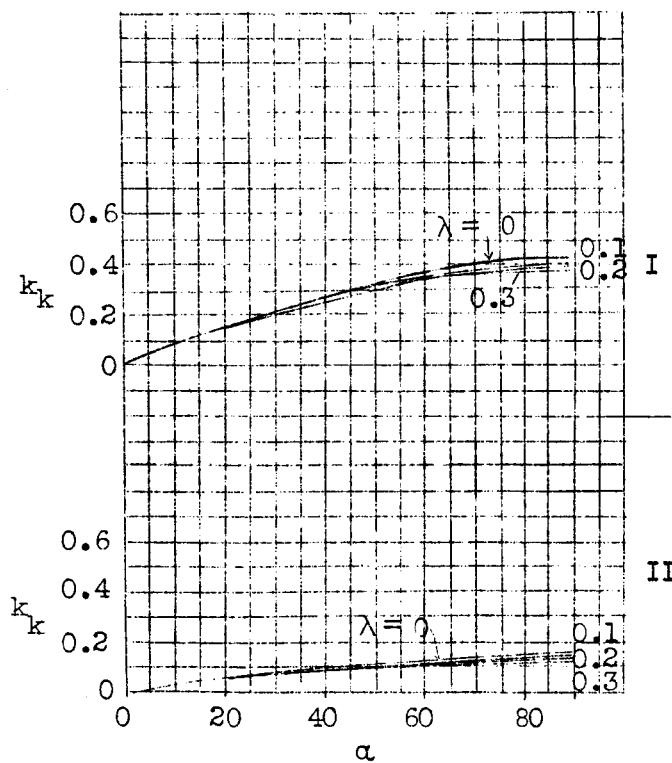


Fig.24  
Moment of yaw  
plotted against  
 $\alpha$

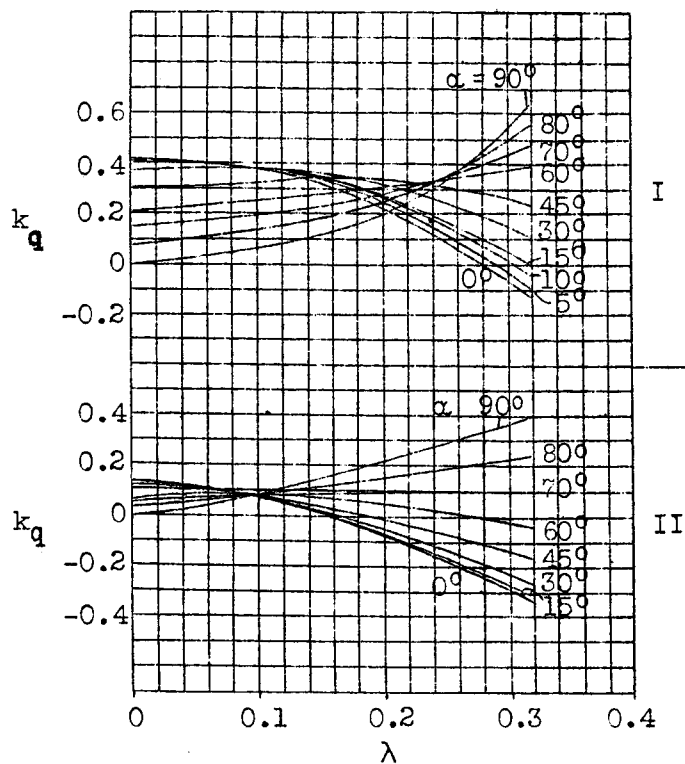


Fig.25  
Lateral moment  
plotted against  
 $\lambda$

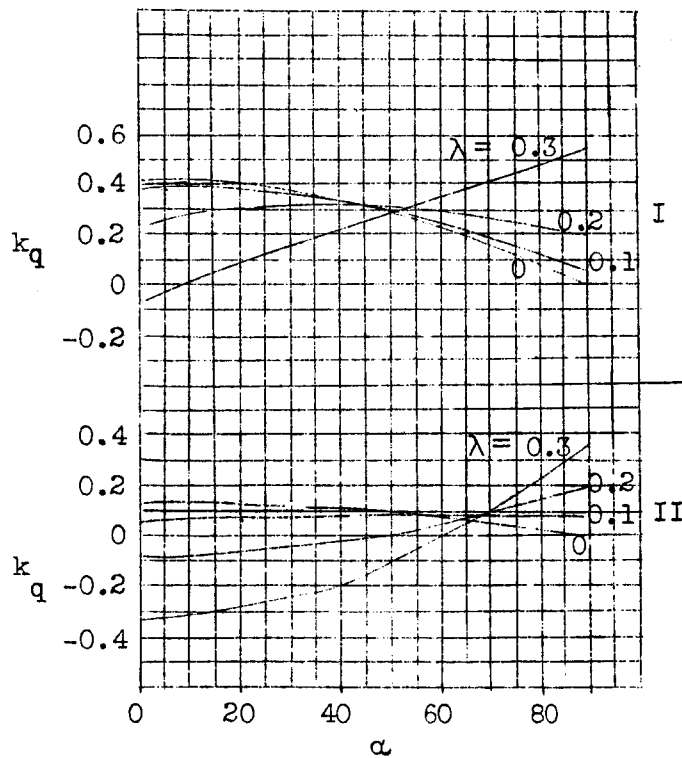


Fig.26  
Lateral moment  
plotted against  
 $\alpha$

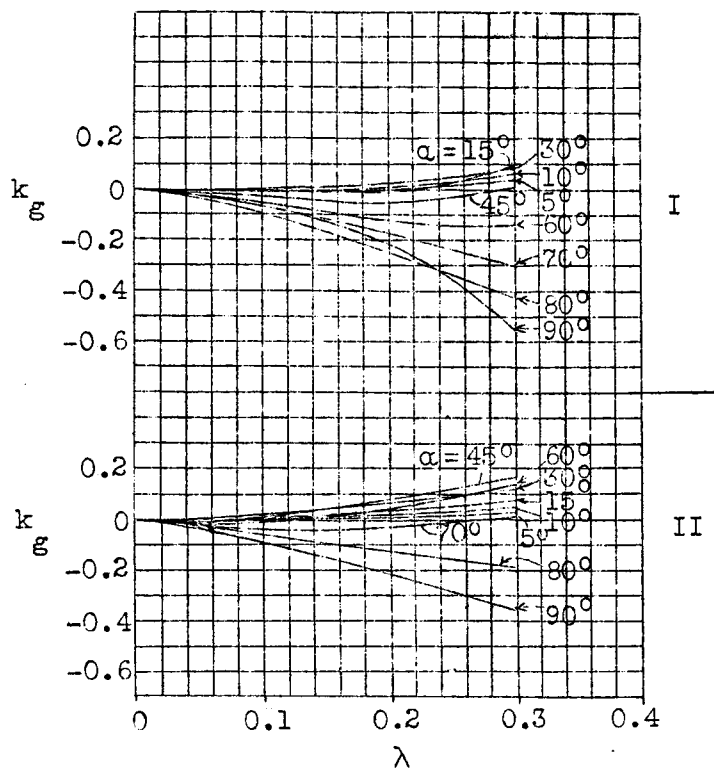


Fig.27  
Moment of yaw  
plotted against  
 $\lambda$

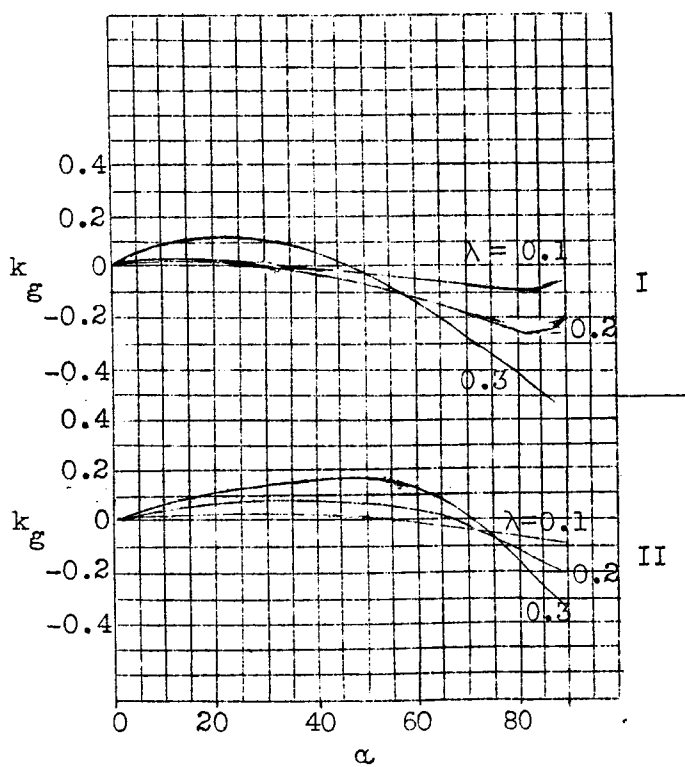


Fig.28  
Moment of yaw  
plotted against  
 $\alpha$

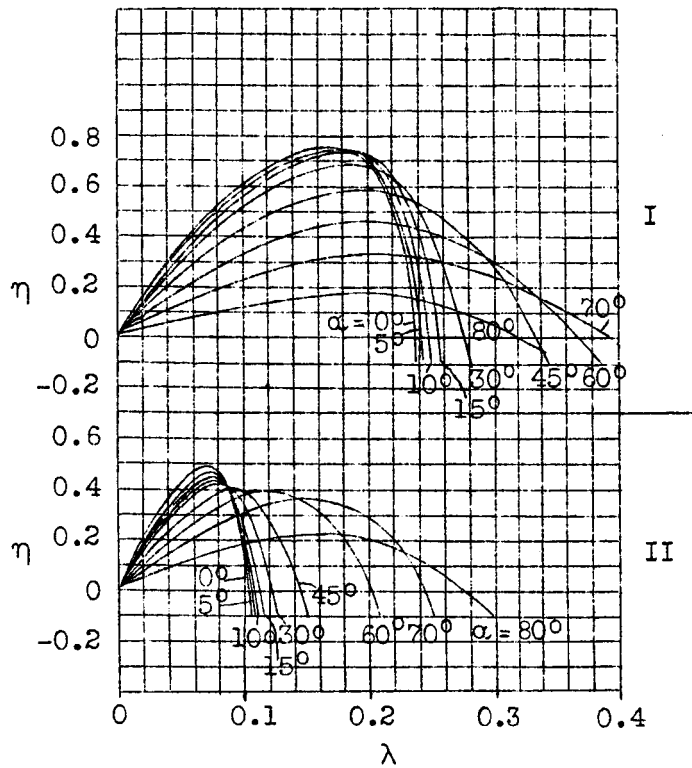


Fig.29  
Propeller efficiency  
plotted against  
 $\lambda$

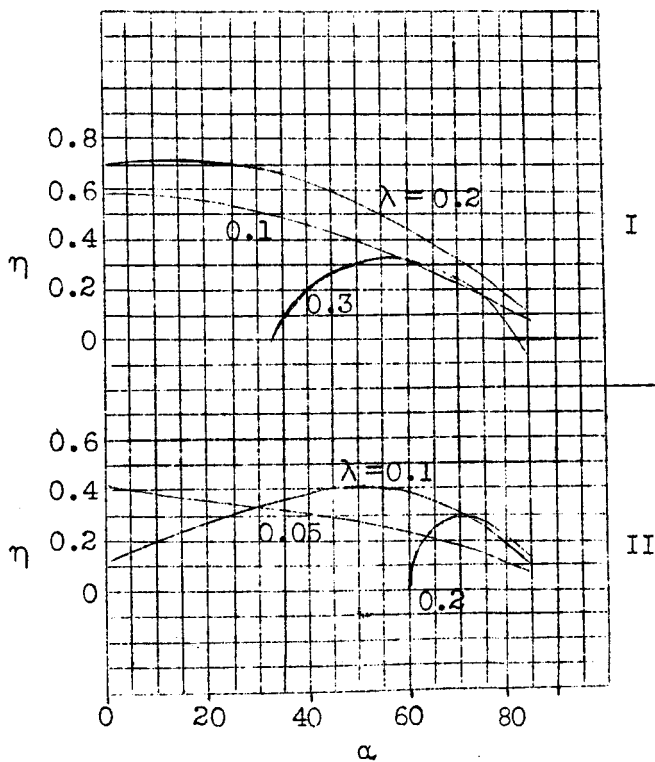


Fig.30  
Propeller efficiency  
plotted against  
 $\alpha$